CRYSTAL GROWTH & DESIGN

Article

pubs.acs.org/crystal

# Precipitation of Ordered Dolomite via Simultaneous Dissolution of Calcite and Magnesite: New Experimental Insights into an Old Precipitation Enigma

G. Montes-Hernandez,*[,†,‡] N. Findling,[‡] F. Renard,[‡,§] and A.-L. Auzende[∥]

[†]CNRS, Institut des Sciences de la Terre (ISTerre), F-38041 Grenoble, France

[‡]Université Grenoble Alpes, ISTerre, F-38041 Grenoble, France

[§]Physics of Geological Processes, University of Oslo, Box 1048 Blindern, 0316 Oslo, Norway

[∥]Institut de Minéralogie et de Physique des Milieux Condensés, CNRS−Université Paris Diderot−UPMC, F-75252 Paris, France

**ABSTRACT:** In the present study, we demonstrate that ordered dolomite can be precipitated via simultaneous dissolution of calcite and magnesite under hydrothermal conditions (from 100 to 200 °C). The temperature and high-carbonate alkalinity have significantly copromoted the dolomite formation. For example, when high-purity water was initially used as interacting fluid, only a small proportion of disordered dolomite was identified at 200 °C from XRD patterns and FESEM observations. Conversely, a higher proportion of ordered dolomite, i.e., clear identification of superstructure ordering reflections in XRD patterns, was determined when high-carbonate alkalinity solution was initially used in our system at the same durations of reaction. For this latter case, the dolomite formation is favorable therefrom 100 °C and two kinetic steps were identified: (1) protodolomite formation after about 5 days of reaction, characterized by rounded submicrometric particles from FESEM observations and by the absence of superstructure ordering reflections at 22.02 (101), 35.32 (015), 43.80 (021), etc. 2$\theta$ in XRD patterns; (2) protodolomite to dolomite transformation, probably produced by a coupled dissolution−recrystallization process. Herein, the activation energy was estimated to be 29 kJ/mol by using a conventional Arrhenius linear equation. This study provides new experimental conditions to which dolomite could be formed in hydrothermal systems. Temperature and carbonate alkalinity are particularly key physicochemical parameters to promote dolomite precipitation in abiotic systems.

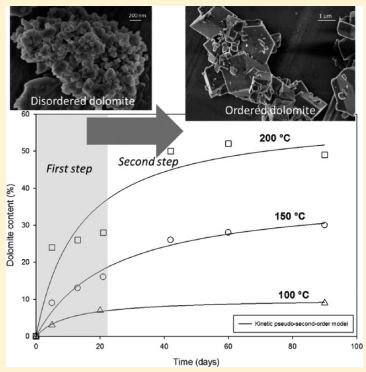


## 1. INTRODUCTION

The formation and textural properties of dolomite ($CaMg(CO_3)_2$) have already been investigated in the past two centuries.[1−4] However, various questions still remain unanswered concerning its formation mechanism and kinetics in natural systems as well as its synthesis in the laboratory. For example, the formation of ordered dolomite at ambient temperature is virtually impossible, possibly due to the high hydration nature of $Mg^{2+}$ ions in solution at low temperature.[4−6] Moreover, the scanty distribution of modern dolomite in nature contrasts strongly with its common abundance in ancient sedimentary rocks of marine origin, leading to the paradox commonly referred to as the "dolomite problem".[7−9] Experimental syntheses regarding the physicochemical conditions, reaction mechanisms, and kinetics at which dolomite can be formed could resolve this paradox. Typically, the dolomite precipitation in the laboratory has been investigated by reference to the natural setting. In this way, three main kinds of experimental configurations have been carried out:

1. The first is direct and homogeneous precipitation by mixing (fast or slowly) two predefined solutions, one containing a Mg/Ca ratio ≥ 1 and the other containing dissolved carbonate ions. This simple reaction pathway has only success at high temperature (>100 °C).[5,10] In a similar way, more sophisticated experimental setups have been built "hydrothermal flow reactors" to investigate the kinetic behavior of dolomite precipitation, but, these systems have systematically used pre-existent dolomite crystals "or seed material", this can indeed provide idealized or limited information on the overgrowth of dolomite (syntaxial and/or epitaxial growth).[9]

2. Calcite dolomitization is carried out by placing high-purity calcite or limestone material in contact with Mg-rich solution. This calcite replacement by ordered dolomite is particularly favorable also at high temperature (>100 °C).[11−13] This reaction mechanism could explain the massive dolomite formation in sedimentary environments if such sediments are submitted to significant temperature variations and/or to significant changes of pore-fluid chemistry over geologic times (see, e.g., ref 14).

3. Bioassisted dolomitization occurs by using sulfate-reducing or aerobic heterotrophic bacteria, hypersaline or seawater solutions, and anoxic or oxic conditions in controlled laboratory

**Received:** October 17, 2013
**Revised:** December 5, 2013

   dx.doi.org/10.1021/cg401548a | *Cryst. Growth Des.* XXXX, XXX, XXX−XXX

**Table 1. Summary of Experimental Conditions and Mineral Content in Solid Products Deduced from Rietveld Refinements of XRD Patterns[a]**

| | | | | | pH | | product amount (%) from XRD | | |
|---|---|---|---|---|---|---|---|---|---|
| run no. | solid reactants | $t$ (days) | $T$ (°C) | solution | initial | final | calcite | magnesite | dolomite |
| 1[b] | $CaCO_3$–$MgCO_3$ | 90 | 50 | HAS | 8.9 | 9.0 | 38 | 57 | 0 |
| 2[b] | $CaCO_3$–$MgCO_3$ | 90 | 75 | HAS | 8.9 | 9.1 | 47 | 49 | 0 |
| 3[b] | $CaCO_3$–$MgCO_3$ | 90 | 100 | HAS | 8.9 | 9.2 | 43 | 43 | 9 |
| 4[b] | $CaCO_3$–$MgCO_3$ | 90 | 150 | HAS | 8.9 | 9.3 | 26 | 40 | 30 |
| 5[c] | $CaCO_3$–$MgCO_3$ | 90 | 200 | HAS | 8.9 | 8.0[d] | 11 | 4 | 49 |
| 6 | $CaCO_3$–$MgCO_3$ | 90 | 50 | PW | ≈6.5 | 10.3 | 61 | 37 | 0 |
| 7 | $CaCO_3$–$MgCO_3$ | 90 | 75 | PW | ≈6.5 | 10.2 | 47 | 52 | 0 |
| 8 | $CaCO_3$–$MgCO_3$ | 90 | 100 | PW | ≈6.5 | 10.0 | 49 | 50 | 0 |
| 9 | $CaCO_3$–$MgCO_3$ | 90 | 150 | PW | ≈6.5 | 9.6 | 27 | 72 | 0 |
| 10 | $CaCO_3$–$MgCO_3$ | 90 | 200 | PW | ≈6.5 | 9.0 | 54 | 39 | 6[e] |
| 11 | $CaCO_3$–$MgCO_3$ | 5 | 150 | HAS | 8.9 | 9.1 | 44 | 45 | 9 |
| 12 | $CaCO_3$–$MgCO_3$ | 13 | 150 | HAS | 8.9 | 9.2 | 56 | 25 | 13 |
| 13 | $CaCO_3$–$MgCO_3$ | 21 | 150 | HAS | 8.9 | 9.2 | 39 | 42 | 16 |
| 14 | $CaCO_3$–$MgCO_3$ | 42 | 150 | HAS | 8.9 | 9.3 | 28 | 38 | 26 |
| 15 | $CaCO_3$–$MgCO_3$ | 60 | 150 | HAS | 8.9 | 9.4 | 28 | 34 | 28 |
| 16 | $CaCO_3$–$MgCO_3$ | 5 | 200 | HAS | 8.9 | 9.2 | 34 | 37 | 24 |
| 17 | $CaCO_3$–$MgCO_3$ | 13 | 200 | HAS | 8.9 | 9.1 | 29 | 40 | 26 |
| 18 | $CaCO_3$–$MgCO_3$ | 21 | 200 | HAS | 8.9 | 9.2 | 39 | 30 | 28 |
| 19 | $CaCO_3$–$MgCO_3$ | 42 | 200 | HAS | 8.9 | 9.1 | 16 | 26 | 50 |
| 20 | $CaCO_3$–$MgCO_3$ | 60 | 200 | HAS | 8.9 | 9.2 | 14 | 21 | 52 |
| 21 | $CaCO_3$–$MgCO_3$ | 5 | 100 | HAS | 8.9 | 9.1 | 46 | 47 | 3 |
| 22 | $CaCO_3$–$MgCO_3$ | 20 | 100 | HAS | 8.9 | 9.0 | 47 | 45 | 6 |

[a]HAS, high-carbonate alkaline solution; PW, high-purity water; $CaCO_3$, calcite; $MgCO_3$, magnesite. [b]For runs 1–4, natrite mineral $NaCO_3$ was also quantified, completing it 100% in solid. [c]For run 5, a microleakage was suspected at the end of experiment; probably this has enhanced the precipitation of eitilite (26%). The pH was measured ex situ at room temperature (≈20 °C). [d]Unrealistic pH. [e]Disordered dolomite.

systems. These complex procedures seem to have success at low temperature to synthesize dolomite as reported in various recent studies;[2,15−18] however, the provided information has not shown convincing proof of the presence of ordered dolomite for these low-temperature syntheses. For example, reported X-ray diffraction (XRD) patterns have not clearly shown the presence of superstructure ordering reflections at 22.02 (101), 35.32 (015), 43.80 (021), etc. $2\theta$ on synthesized material as described by Lippmann.[19] Moreover, the reaction mechanism and role of all parameters (including culture media and/or cellular secretions) is poorly understood. Identifying novel and/or innovative abiotic or biotic synthesis methods for dolomite in a broad spectrum of experimental conditions still remains a major scientific challenge to obtain a better understanding of its formation in natural systems and to facilitate its production at the laboratory scale.

In this context, the present study has explored a new synthesis pathway for dolomite by using calcite and magnesite as Ca and Mg sources, respectively ($CaCO_3 + MgCO_3 \rightarrow CaMg(CO_3)_2$). This reaction pathway has not been investigated to the best of our knowledge. However, calcite and magnesite could coexist in various natural media (sedimentary deposits, modern marine sediments, hydrothermal systems, deep geological formations, etc.). Moreover, this simple reaction pathway allows us to determine if dolomite formation is favorable via dissolution of its Mg-rich and Ca-rich end members under hydrothermal conditions in closed systems.

## 2. MATERIALS AND METHODS

**2.1. Preparation of Solid Reactants.** *Calcite.* High-purity calcite characterized by nanosized (<100 nm) and submicrometric (<1 μm) particles were synthesized by aqueous carbonation of portlandite ($Ca(OH)_2$). The specific procedure and fine calcite characterization have already been reported by Montes-Hernandez et al.[20]

*Magnesite.* Rhombohedral single crystals (<2 μm) of magnesite were synthesized by two main sequential reactions: (1) aqueous carbonation of synthetic brucite ($Mg(OH)_2$) by injection of $CO_2$ in a highly alkaline medium (2 *m* NaOH) at ambient temperature (~20 °C), leading to precipitation of platy-compacted aggregates of dypingite ($Mg_5(CO_3)_4(OH)_2{\cdot}5H_2O$) after 24 h; (2) complete dypingite-to-magnesite transformation after 24 h by a simple heat-aging step from 20 to 90 °C. These synthesis pathways and magnesite characterizations have been previously reported by Montes-Hernandez et al.[21]

**2.2. Preparation of Reacting Solutions.** High-purity water with an electrical resistivity of 18.2 MΩ cm (PW) and high-carbonate alkaline solution (HAS) were used as interacting solutions in the dolomitization experiments. The HAS was prepared by direct capture of $CO_2$ in contact with a concentrated NaOH solution (2 *m*). Herein, 50 bar of $CO_2$ (~2 mol) was injected into the titanium reaction cell (2 L volume) at ambient temperature (~20 °C). The $CO_2$ consumption (or pressure drop of $CO_2$) and temperature (exothermic reaction) were in situ monitored until a macroscopic equilibrium that was reached after about 24 h. Then, the residual $CO_2$ gas was removed from the reactor and the solution was recovered by simple decanting of the supernatant solution. Based on Solvay typical reactions, the following global reactions are expected:

$$2NaOH + CO_2 \rightarrow Na_2CO_3 + H_2O \quad (1a)$$

$$Na_2CO_3 + H_2O + CO_2 \rightarrow 2NaHCO_3 \quad (1b)$$

The X-ray diffraction on the recovered solid and the measurements in the solution (pH 8.7 and total carbon (TC) = 0.95 M) have confirmed reactions 1a and 1b.

**2.3. Dolomitization Experiments.** Five Teflon reaction cells were loaded with 1.5 mL of high-carbonate alkaline solution (HAS), 100 mg of calcite, and 100 mg of magnesite. Five other reaction cells were loaded with the same mineral amounts, but with 1.5 mL of high-


dx.doi.org/10.1021/cg401548a | Cryst. Growth Des. XXXX, XXX, XXX−XXX

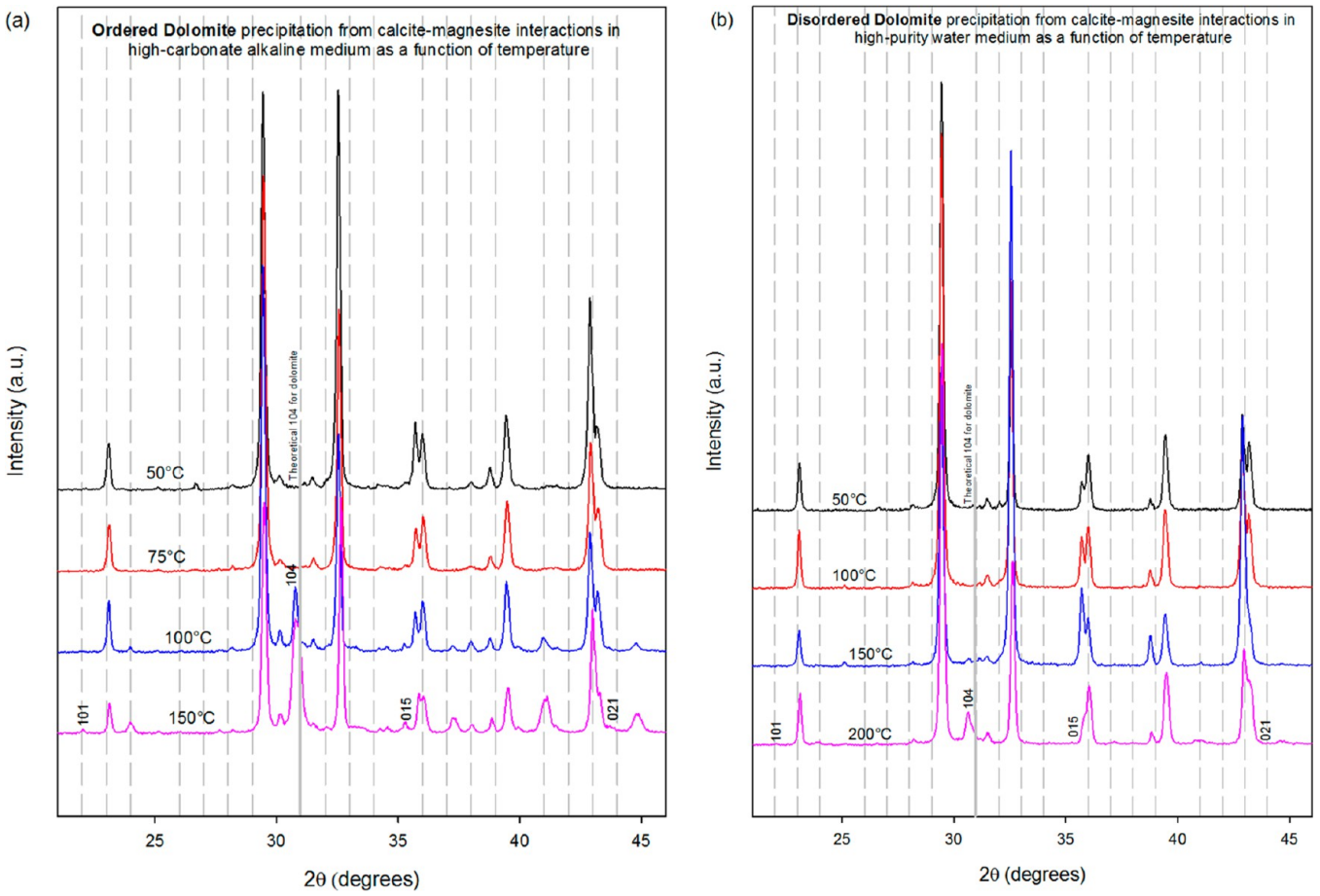


**Figure 1.** Experimental XRD patterns for dolomite precipitation via simultaneous dissolution of calcite and magnesite. 101, 015, and 021 are typical superstructure reflections for dolomite in the 20−45 2$\theta$ range (ICDD 036-0426). Influence of temperature and nature of interacting fluid. (a) Reaction in high-carbonate alkaline solution and (b) in high-purity water.

purity water (PW). All reaction cells (cap cell also in Teflon) were immediately assembled into independent steel mini autoclaves without agitation, referred to as the "static batch reactor" and the closed autoclaves were placed in a multioven (10 independent temperature compartments). This allowed the simultaneous investigation of five independent temperatures (50, 75, 100, 150, and 200 °C) and two different interacting solutions (PW and HAS). The reaction duration for these 10 experiments was arbitrarily imposed as 90 days. These exploratory experiments have revealed that ordered dolomite is preferentially formed in carbonate alkaline medium therefrom 100 °C for the investigated lapse of time. For this reason, complementary dolomitization experiments were performed using exclusively carbonate alkaline solution as interacting fluid in order to determine the dolomite precipitation rate. For this case, five reaction durations were arbitrarily imposed (5, 13, 21, 42, and 62 days) at three different temperatures (100, 150, and 200 °C). We note that only two reaction durations (5 and 20 days) were considered for experiments at 100 °C. In all experiments, the same mineral amounts of reactants and volume of interacting solution were used. All experiments and some results are summarized in Table 1. At the end of the experiment, the autoclave was quenched in cold water. This manipulation limits a significant perturbation of the solid reaction products with respect to a slow cooling process. Then, the autoclave was disassembled and the fluid was collected for pH measurement exclusively. Finally, the solid product was directly dried in the Teflon reaction cells at 90 °C for 24 h. The dry solid product was recovered for further solid characterizations described in section 2.4.

**2.4. Characterization of Solid Products.** X-ray powder diffraction (XRD) analyses were performed using a Siemens D5000 diffractometer in Bragg−Brentano geometry; equipped with a $\theta$−$\theta$ goniometer with a rotating sample holder. The XRD patterns were collected using Cu K$\alpha_1$ ($\lambda_{K\alpha_1}$ = 1.5406 Å) and Cu K$\alpha_2$ ($\lambda_{K\alpha_2}$ = 1.5444 Å) radiation in the range 2$\theta$ = 10−70° with a step size of 0.04° and a counting time of 6 s per step. Residual calcite and magnesite, dolomite, and natrite minerals in XRD patterns were systematically refined by the Rietveld method using BGMN software and its associated database,[22] except for run 5 where eitelite mineral was also added. The precipitation of this latter mineral was probably promoted by an unexpected microleakage in the system, which was confirmed at the end of the experiment.

*Field Emission Scanning Electron Microscopic (FESEM) Observations.* Selected samples containing dolomite were dispersed by ultrasonic treatment in absolute ethanol for 5−10 min. One or two droplets of the suspension were then deposited directly on an aluminum support for SEM observations, and coated with platinum. The morphology of crystal faces was observed by using a Zeiss Ultra 55 field emission gun scanning electron microscope (FESEM) with a maximum spatial resolution of approximately 1 nm at 15 kV.

*Transmission Electron Microscopic (TEM) Observations.* One selected sample (from run 16) was shaken in ethanol for a short time in order to split the aggregates without any additional treatment. A drop of the suspension was deposited on a holey carbon foil and placed on a conventional copper microgrid for further observations with a JEOL 2100F transmission electron microscope (TEM) operating at 200 kV, equipped with a field emission gun and a high-resolution pole piece achieving a point-to-point resolution of 1.8 Å. Chemical mapping was achieved by combining the scanning module of the microscope (STEM) with the energy dispersive spectroscopic (EDS) detector.


dx.doi.org/10.1021/cg401548a | *Cryst. Growth Des.* XXXX, XXX, XXX−XXX

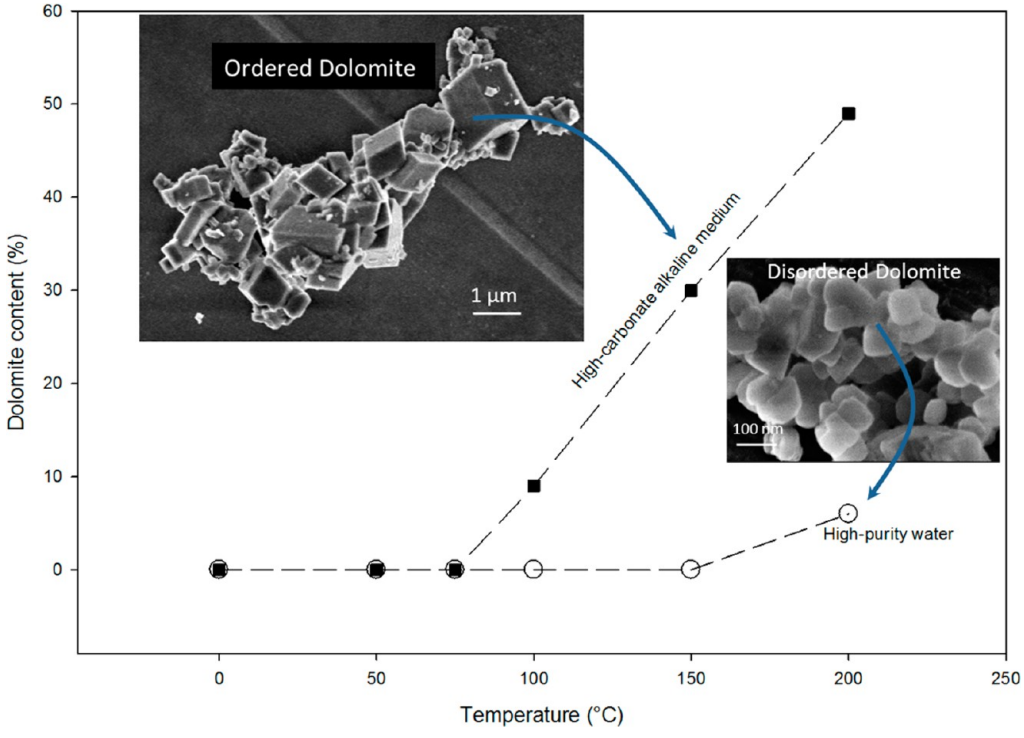


**Figure 2.** Dolomite content behavior as a function of temperature for two different initial interacting fluids (high-carbonate alkaline solution and high-purity water). Dolomite content was deduced from Rietveld refinement of XRD patterns shown in Figure 1. Insets: FESEM microimages showing ordered and disordered dolomite morphologies.

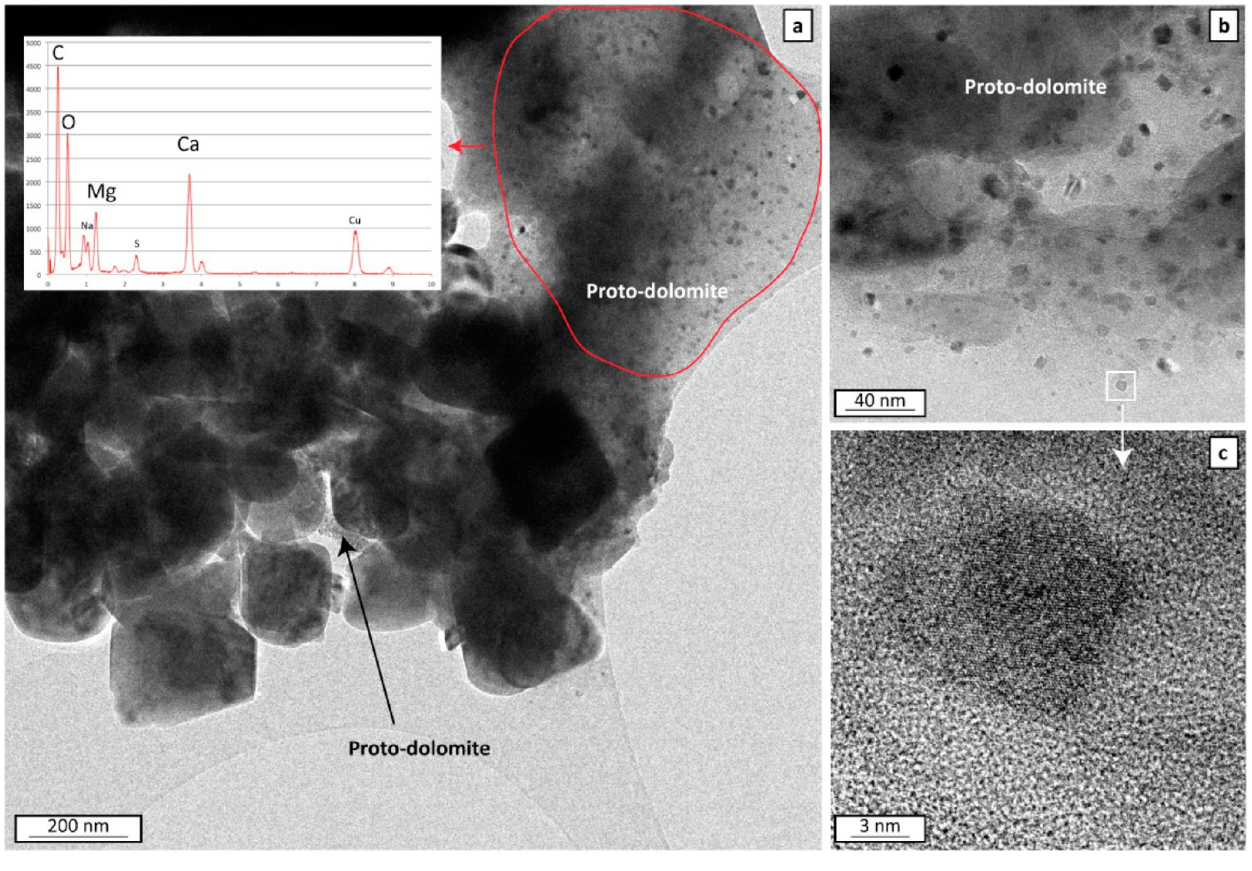


**Figure 3.** (a) Bright field image of protodolomite mixed with calcite and magnesite grains (from run 16) (inset: EDS spectrum extracted from STEM chemical mapping); (b) magnification of protodolomite where nanoparticles are scattered in an amorphous gel; (c) high-resolution image of a crystalline nanoparticle.


dx.doi.org/10.1021/cg401548a | *Cryst. Growth Des.* XXXX, XXX, XXX−XXX

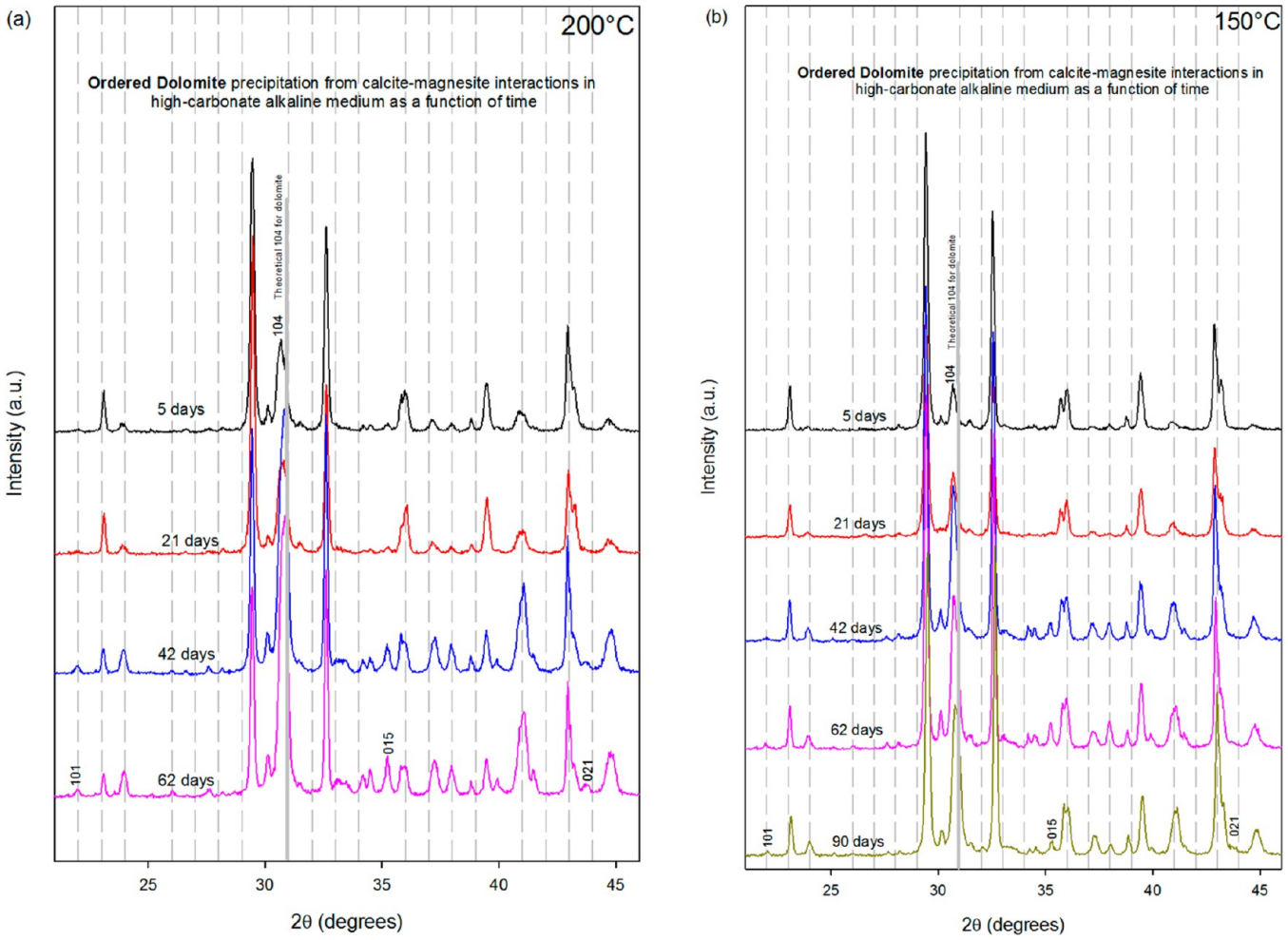


**Figure 4.** Experimental XRD patterns for dolomite precipitation via simultaneous dissolution of calcite and magnesite. 101, 015, and 021 are typical superstructure reflections for dolomite in the 20−45 2$\theta$ range (ICDD 036-0426). Kinetic behavior at (a) 200 and (b) 150 °C.

*Thermogravimetric Analysis.* TGA for all solid products was performed with a Mettler Toledo TGA/SDTA 851e instrument under the following conditions: sample mass of about 10 mg, 150 $\mu$L alumina crucible with a pinhole, heating rate of 10 °C min$^{-1}$, and inert $N_2$ atmosphere of 50 mL min$^{-1}$. We note that all samples containing dolomite were also analyzed under a $CO_2$ atmosphere using the same flow (50 mL/min) in order to separate correctly the dolomite decomposition from magnesite and calcite decomposition in the samples. Sample mass loss and associated thermal effects were obtained by TGA/simultaneous differential thermal analysis (SDTA). In order to identify the different mass loss steps, the TGA first derivative (rate of mass loss) was used. The TGA apparatus was calibrated in terms of mass and temperature. Calcium oxalate was used for the sample mass calibration. The melting points of three compounds (indium, aluminum, and copper) obtained from the DTA signals were used for the sample temperature calibration.

## 3. RESULTS AND DISCUSSION

Under Earth's surface conditions, calcite and magnesite are the most stable carbonates containing calcium and magnesium, respectively. Assuming that these two minerals could coexist in hydrothermal systems and other Earth or planetary systems, this study provides new experimental conditions to which the dolomite can be formed via simultaneous dissolution of calcite and magnesite. Obviously, this particular case could not explain the dolomite abundance in ancient sedimentary rocks of marine origin.

**Table 2. Summary of Kinetic Parameters for Dolomite Formation via Simultaneous Dissolution of Calcite and Magnesite in High-Carbonate Alkaline Medium[a]**

| temp (°C) | $\xi_{extent,\ max}$ (%) | $t_{1/2}$ (days) | $v_0$ (1/day) | $E_a$ (kJ/mol) |
|---|---|---|---|---|
| | $CaCO_3 + MgCO_3 \rightarrow CaMg(CO_3)_2$ | | | |
| 100 | 10.7 | 17.8 | $6.01 \times 10^{-3}$ | |
| 150 | 38.5 | 23.8 | $1.61 \times 10^{-2}$ | 29 |
| 200 | 59.4 | 13.5 | $4.40 \times 10^{-2}$ | |

[a] $\xi_{extent,max}$ is the maximum value of dolomite content at apparent equilibrium, and $t_{1/2}$ is the half-content time determined by using a kinetic pseudo-second-order model. $v_0$ is the initial reaction rate ($v_0 = \xi_{extent,max}/t_{1/2}\cdot 100$). $E_a$ is the activation energy determined by the Arrhenius equation (conventional linear form).

X-ray diffraction results have revealed the formation of ordered dolomite therefrom 100 °C when high-carbonate alkaline solution was used as interacting fluid. This was clearly identified by the presence of superstructure ordering reflections 101, 015, 021, etc. from the ICDD 036-0426 pattern for dolomite (Figure 1). Conversely, a small proportion of disordered dolomite was exclusively identified at 200 °C when high-purity water was used as interacting fluid for the same duration of reaction (90 days) (Figure 1b). Electron microscopy observations (FESEM) have shown rounded submicrometric particles for disordered dolomite and rhombo-


dx.doi.org/10.1021/cg401548a | Cryst. Growth Des. XXXX, XXX, XXX−XXX

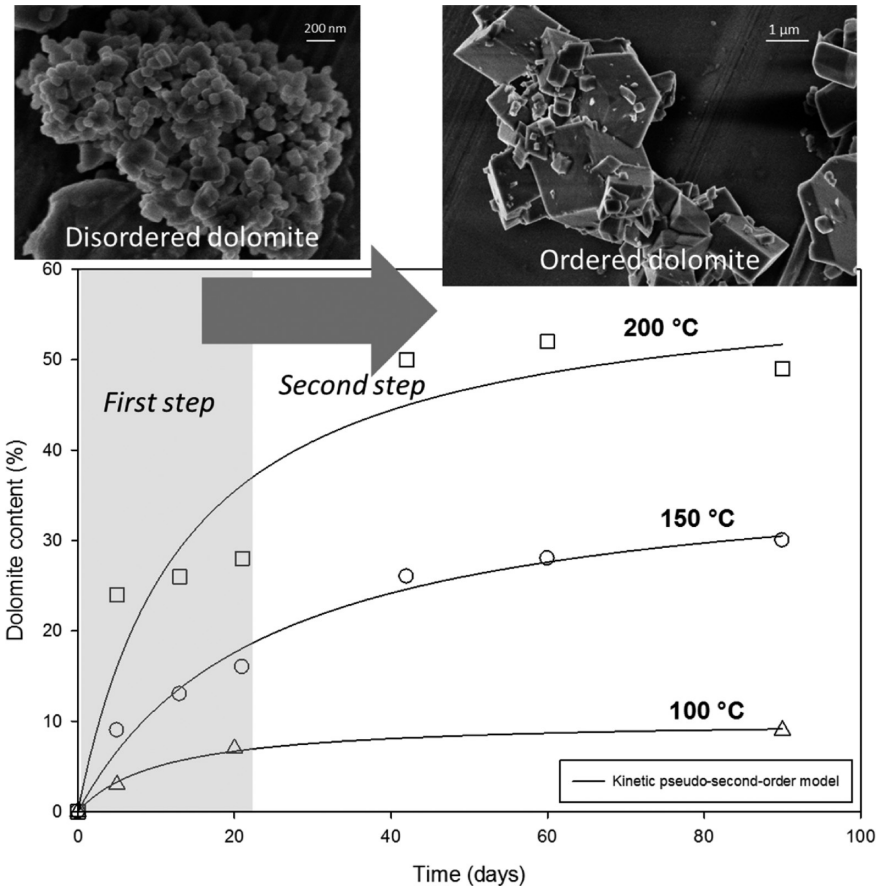


**Figure 5.** Temperature influence on the kinetic of dolomite formation via simultaneous dissolution of calcite and magnesite in high-carbonate medium. Dolomite content was deduced from Rietveld refinement of XRD patterns shown in Figure 3. Insets: FESEM microimages show that disordered dolomite is first formed followed by the formation of ordered dolomite (slower step).

hedral micrometric particles for ordered dolomite (see insets in Figure 2). These morphologies are not surprising results because rounded submicrometric particles have been also identified from laboratory bioassisted experiments at low temperature (see, e.g., refs 2, 17, and 23), and rhombohedral morphology is typical for ordered dolomite from natural Earth systems or synthesized under hydrothermal conditions via mineral replacement of calcite (see, e.g., ref 24).

Figure 2 summarizes the dolomite content as a function of temperature. The dolomite content was deduced from Rietveld refinements of XRD patterns. When high-carbonate alkalinity was used, the dolomite content in solid products seems to be directly proportional to temperature from 100 to 200 °C. However, dolomite was not detected at 50 and 75 °C for the same reaction duration. The dolomitization process is limited via simultaneous hydrothermal dissolution in high-purity water. In fact, a small proportion of dolomite (6%) was only determined at 200 °C for a reaction duration of 90 days. On the basis of these exploratory results, we assume that formation of dolomite via simultaneous dissolution of calcite and magnesite is significantly copromoted by temperature and high-carbonate alkalinity. We note that carbonate alkalinity has been suspected to increase significantly in bioassisted dolomite synthesis at low temperature (see, e.g., refs 2, 15, and 16) or in natural systems,[8,25] but this parameter is not enough to promote alone the dolomite formation in abiotic systems at low temperature (<100 °C) via simultaneous dissolution of calcite and magnesite, probably because both minerals remain stable in high-carbonate alkaline medium. However, this original result opens new possibilities for investigating dolomite formation in abiotic systems at low temperature, obviously, by using soluble salts as Ca and Mg sources.

Considering now that dolomite formation is promoted in high-carbonate alkaline medium therefrom 100 °C, complementary dolomitization experiments were performed at five different reaction durations (5, 13, 21, 42, and 60 days) and three different temperatures (100, 150, and 200 °C) in order to assess the dolomitization rate and reaction mechanism. In this way, two kinetic steps were clearly identified:

1. Rapid protodolomite formation occurred by simultaneous dissolution of calcite and magnesite (or disordered dolomite—the absence of superstructure reflections 101, 015, 021, etc.), dominant in the first 20 days and positively correlated with temperature. In fact, the protodolomite is a nanocrystalline phase (see Figure 3) which contains a very high Mg atomic concentration (>38%), but an irregular intercalation between Ca and Mg into the crystals is only expected as clearly determined by XRD (Figure 4).

2. The second kinetic step was the protodolomite to dolomite transformation, probably by a coupled dissolution–recrystallization process. This second step remains still an open question for dolomite formation in our experiments, but it seems dominant therefrom 20 days of reaction as clearly identified in experimental XRD patterns (see Figure 4). On the basis of XRD patterns and some TEM observations, we suggest that the so-called protodolomite is rapidly transformed to


dx.doi.org/10.1021/cg401548a | Cryst. Growth Des. XXXX, XXX, XXX–XXX

ordered dolomite, but both crystalline phases can coexist as a function of time if Ca and Mg sources are still available. This is in agreement with a suspected overlapping in 104 peaks. Consequently, it is very difficult to determine if an evolution of the order degree exists during dolomite formation in our experiments.

The temporal variation of dolomite content was determined from Rietveld refinements of XRD patterns. These experimental kinetic data were then fitted by using a simple kinetic model (kinetic pseudo-second-order model) in order to estimate the initial reaction rate of dolomitization. Graphically, this initial rate is defined as the slope of the tangent line when the time tends toward zero on the "dolomite content versus time" curve.[20] The results summarized in Table 2 reveal that the initial reaction rate of dolomitization and the maximum of dolomite content are positively correlated with temperature (see Figure 5 and Table 2). This temperature dependence suggests an agreement with Arrhenius' law, which allows a simple estimation of the activation energy ($E_a$ = 29 kJ/mol) for dolomitization reaction in our experiments. This value is about 4 times lower than the value of 133.3 kJ/mol reported by Arvidson and Mackenzie.[8,9] The experimental configurations are not necessarily comparable; however, we assume that the high-carbonate alkalinity decreases significantly the energetic barriers to form dolomite in a given system.

The results deduced from the Rietveld refinements of XRD patterns were compared with thermogravimetric (TG) measurements performed in 100% $N_2$ or $CO_2$ atmosphere. The results obtained from both analytical techniques are generally in agreement, except for lower dolomite contents in the solid products. Herein, the dolomite decomposition, concerning the first step ($CaMg(CO_3)_2 \rightarrow MgO + CaCO_3$) during the heating process, was systematically overlapped with magnesite decomposition in both gas atmospheres, with magnesite decomposition starting at a lower temperature. For this specific study, we assumed that Rietveld refinement of XRD patterns is better adapted to estimate the dolomite content in synthesized solids.

Calcite and magnesite could coexist in various active natural media (sedimentary deposits, modern marine sediments, hydrothermal systems, deep geological formations, etc.0. On the basis of the above results, the calcite−magnesite interactions in alkaline media could represent a potential source of dolomite. At the present time, this scenario has not been considered in the geosciences to the best of our knowledge.

## 4. CONCLUSION

This study provides new experimental conditions to which dolomite can be formed in hydrothermal systems via simultaneous dissolution of calcite and magnesite. Herein, the dolomite formation was copromoted by temperature and high-carbonate alkalinity. The activation energy for this reaction pathway ($CaCO_3 + MgCO_3 \rightarrow CaMg(CO_3)_2$) is 29 kJ/mol. This reaction pathway has not been documented in the literature; however, it could exist in deep geological formations and/or hydrothermal systems. In conclusion, this basic research opens new possibilities for investigating abiotic formation of dolomite at the laboratory scale, probably toward the abiotic formation of dolomite at low temperature (<100 °C).

## AUTHOR INFORMATION

### Corresponding Author

*E-mail: german.montes-hernandez@ujf-grenoble.fr.

### Notes

The authors declare no competing financial interest.

## ACKNOWLEDGMENTS

The authors are grateful to the French National Center for Scientific Research (CNRS), the Université Grenoble Alpes, the Labex OSUG@2020 (Investissement d'avenir-ANR10-LABX56), and the ANR French research agency (ANR CORO and ANR SPRING projects) for providing financial support.

## REFERENCES

(1) McKenzie, J. A. The dolomite problem: an outstanding controversy. In *Controversies in Modern Geology: Evolution of Geological Theories in Sedimentology*; Muller, D. W., McKenzie, J. A., Weissert, H., Eds.; Academic Press: London, 1991; pp 37−54.
(2) Sanchez-Roman, M.; McKenzie, J. A.; Wagener, A-de-L. R.; Rivadeneyra, M. A.; Vasconcelos, C. *Earth Planet. Sci. Lett.* **2009**, *285*, 131.
(3) McKenzie, J. A.; Vasconcelos, C. *Sedimentology* **2009**, *56*, 205.
(4) Deelman, J. C. *Low-Temperature Formation of Dolomite and Magnesite*; 2011; pp 211−273. http://www.jcdeelman.demon.nl/dolomite/bookprospectus.html.
(5) Deelman, J. C. *Chem. Erde* **2001**, *61*, 224.
(6) Xu, J.; Yan, C.; Zhang, F.; Konishi, H.; Xu, H.; Teng, H. *Proc. Natl. Acad. Sci. U.S.A.* **2013**, *110*, 17750 DOI: 10.1073/pnas.1307612110.
(7) Compton, J. S. *Geology* **1988**, *16*, 318.
(8) Arvidson, R. S.; Mackenzie, F. T. *Aquat. Geochem.* **1997**, *2*, 273.
(9) Arvidson, R. S.; Mackenzie, F. T. *Am. J. Sci.* **1999**, *299*, 257.
(10) Medlin, W. L. *Am. Mineral.* **1959**, *44*, 979.
(11) Grover, J.; Kubanek, F. *Am. J. Sci.* **1983**, *283*, 514.
(12) Dockal, J. *Carbonates Evaporites* **1988**, *3*, 125.
(13) Kaczmarek, S.; Sibley, D. F. *Sediment. Geol.* **2011**, *240*, 30.
(14) Warren, J. *Earth-Sci. Rev.* **2000**, *52*, 1.
(15) Warthmann, R.; Van Lith, Y.; Vasconcelos, C.; McKenzie, J. A.; Karpoff, A. M. *Geology* **2000**, *28*, 1091.
(16) Kenward, P. A.; Goldstein, R. H.; Gonzalez, L. A.; Roberts, J. A. *Geobiology* **2009**, *7*, 556.
(17) Deng, S.; Dong, H.; Lv, G.; Jiang, H.; Yu, B.; Bishop, E. *Chem. Geol.* **2010**, *278*, 151.
(18) Krause, S.; Liebetrau, V.; Gorb, S.; Sanchez-Roman, M.; Mackenzie, J. A.; Treude, T. *Geology* **2012**, *40*, 587.
(19) Lippmann, F. *Sedimentary Carbonate Minerals*; Springer-Verlag: Berlin, 1973; 228 pp.
(20) Montes-Hernandez, G.; Fernandez-Martinez, A.; Renard, F. *Cryst. Growth Des.* **2009**, *9*, 4567.
(21) Montes-Hernandez, G.; Renard, F.; Chiriac, R.; Findling, N.; Toche, F. *Cryst. Growth Des.* **2012**, *12*, 5233.
(22) Taut, T.; Kleeberg, R.; Bergmann, J. *Mater. Struct.* **1998**, *5*, 57.
(23) Perri, E.; Tucker, M. E. *Geology* **2007**, *35*, 207.
(24) Malone, M. J.; Baker, P. A.; Burns, S. J. *Geochim. Cosmochim. Acta* **1996**, *60*, 2189.
(25) Katz, A.; Matthews, A. *Geochim. Cosmochim. Acta* **1977**, *41*, 297.